


Entropy production and entropy extraction rates for a Brownian particle that walks in underdamped medium

Mesfin Asfaw Taye*

Science Division, West Los Angeles College, 9000 Overland Ave., Culver City, California 90230, USA

 (Received 2 November 2019; revised manuscript received 19 December 2019; published 28 January 2020)

The expressions for entropy production, free energy, and entropy extraction rates are derived for a Brownian particle that walks in an underdamped medium. Our analysis indicates that as long as the system is driven out of equilibrium, it constantly produces entropy at the same time it extracts entropy out of the system. At steady state, the rate of entropy production \dot{e}_p balances the rate of entropy extraction \dot{h}_d . At equilibrium both entropy production and extraction rates become zero. The entropy production and entropy extraction rates are also sensitive to time. As time progresses, both entropy production and extraction rates increase in time and saturate to constant values. Moreover, employing microscopic stochastic approach, several thermodynamic relations for different model systems are explored analytically and via numerical simulations by considering a Brownian particle that moves in overdamped medium. Our analysis indicates that the results obtained for underdamped cases quantitatively agree with overdamped cases at steady state. The fluctuation theorem is also discussed.

DOI: [10.1103/PhysRevE.101.012131](https://doi.org/10.1103/PhysRevE.101.012131)

I. INTRODUCTION

Exploring the thermodynamic feature of equilibrium systems is vital and recently has received significant attention since these systems serve as a starting point to study the thermodynamic properties of systems which are far from equilibrium. Because most physically relevant systems are far from equilibrium, it is vital to explore the thermodynamic properties of systems which are driven out of equilibrium. However, such systems are often challenging since their thermodynamic relations such as entropy and free energy depend on their reaction rates. Despite the challenge, the thermodynamic relations of systems which are far from equilibrium are explored in the works in [1–4]. Particularly, the Boltzmann-Gibbs nonequilibrium entropy along with the entropy balance equation serve as an important tool to explore the nonequilibrium thermodynamic features [1–3].

In the past, microscopic stochastic approach has been used by Schnakenberg to derive various thermodynamic quantities such as entropy production rate in terms of local probability density and transition probability rate [3]. Later, many theoretical studies were conducted; see, for example, the works in [4–16]. Recently, we presented an exactly solvable model and studied the factors that affect the entropy production and extraction rates [17–19] for a Brownian particle that walks on a discrete lattice system. More recently, using Boltzmann-Gibbs nonequilibrium entropy, we derived the general expressions for the free energy, entropy production, and entropy extraction rates for a Brownian particle moving in a viscous medium where the dynamics of its motion is governed by the Langevin equation. Employing Boltzmann-Gibbs nonequilibrium entropy as well as from the knowledge of local probability

density and particle current, it is shown that as long as the system is far from equilibrium, it constantly produces entropy and at the same time extracts entropy out of the system. Since many biological problems such as intracellular transport of kinesin or dynein inside the cell can be studied by considering a simplified model of particles walking on lattice as discussed in works by Bameta *et al.* [20], Oriola *et al.* [21], and Campas *et al.* [22], the model considered will serve as a starting point to study the thermodynamics features of two or more interacting particles hopping on a lattice. At this point, it is important to stress that most of our studies are focused on exploring the thermodynamic property of systems that operate in the classical regimes. For systems that operate at quantum realm, the dependence of thermodynamic quantities on the model parameters is studied in the works in [23–25]. Particularly, Boukobza *et al.* investigated the thermodynamic feature of a three-level maser. Not only the entropy production rate is defined in terms of the system parameters but it is shown that the first and second laws of thermodynamics are always satisfied in the model system [25].

In this work, using Langevin equation and Boltzmann-Gibbs nonequilibrium entropy, the general expressions for the free energy, entropy production \dot{e}_p , and entropy extraction rates \dot{h}_d are derived in terms of velocity and probability distribution considering a Brownian particle that moves in underdamped medium. Moreover, after extending the results obtained by Tome *et al.* [26] to a spatially varying temperature case, we further analyze our model systems. We show that the approximation performed based on Tome *et al.* [26] and our general analytic expression agree exactly. The analytic results also justified via numerical simulations. The main results obtained in this work depict that in the absence of load, the entropy production rate decreases as time increases and, in the long time limit, it approaches zero while the entropy extraction rate always approaches zero regardless of time

*tayem@wlaac.edu

t . The above shown results can be explained intuitively on physical bases. As one can note that, for the isothermal case, in the long time limit the system reaches stationary state. If the change in entropy $\Delta S(t)$ is taken while the system is at the stationary state, then $\Delta S = 0$ or $\Delta e_p = 0$. However, since the system operates irreversibly while operating at a finite time (far from the quasistatic limit), the second law of thermodynamics states that $\Delta S(t) > 0$. In fact, the results of this work depict that when the particle relaxes to its equilibrium state, it produces entropy and, if the change in these parameters is taken between $t = 0$ and any time t , always the inequality $\Delta S(t) = S(t) - S(0) > 0$ holds true and as time progresses the change in these parameters increases. Moreover, it is found that, at stationary state, the entropy production and extraction rates approach zero either the particle operates in underdamped or overdamped medium.

To explore how the various thermodynamic relations behave when the system does work against the load f , the dependence of the thermodynamic relations on the load f is explored. In the presence of nonzero force, it is shown that the entropy production and extraction rates increase in time and saturate to a constant value. The fact that the entropy production and extraction rates are greater than zero indicates that the system is out of equilibrium since the system does work at a finite time. At small t , $\dot{e}_p(t) > \dot{h}_d(t)$ revealing that, even if at steady state $\dot{e}_p(t) = \dot{h}_d(t)$, the system produces an enormous amount of entropy at initial time and in latter time or any time t , $\Delta e_p(t) > \Delta h_d(t)$, revealing $\Delta S(t) > 0$ which is a vivid indication that the second law of thermodynamics is always preserved.

Furthermore, we discuss the nonequilibrium thermodynamic features of a Brownian particle that hops in a ratchet potential where the potential is coupled with a spatially varying temperature. It is shown that the operational regime of such a Brownian heat engine is dictated by the magnitude of the external load f . The steady state current or equivalently the velocity of the engine is positive when f is smaller and the engine acts as a heat engine. In this regime $\dot{e}_p = \dot{h}_d > 0$. When f increases, the velocity of the particle decreases and, at stall force, we find that $\dot{e}_p = \dot{h}_d = 0$ showing that the system is reversible at this particular choice of parameter. For large load, the current is negative and the engine acts as a refrigerator. In this region $\dot{e}_p = \dot{h}_d < 0$. Here we first study the underdamped case via simulations and then, for the overdamped case, the thermodynamic feature for the model system is explored analytically. The main result indicates that, in the regime where the velocity is high, the entropy production and extraction rates are also significantly high.

The rest of paper is organized as follows. In Sec. II, we present the model system as well as the derivation of entropy production and free energy. In Sec. III, we explore the dependence for the entropy production, entropy exaction, and free energy rates on the system parameters for a Brownian particle that freely diffuses in an isothermal underdamped medium. In Sec. IV, the dependence for various thermodynamic quantities on system parameters is explored considering a Brownian particle that undergoes a biased random walk in a spatially varying thermal arrangement in the presence of external load. In Sec. V, we consider a Brownian particle walking in ratchet potential. The fluctuation theorem is

discussed in Sec. VI. Section VII deals with summary and conclusion.

II. FREE ENERGY AND ENTROPY PRODUCTION

In the work in [26], the expressions for entropy production and entropy extraction rates were presented in terms of particle velocity and probability distribution considering underdamped and isothermal medium. For a spatially varying thermal arrangement, next we derive the thermodynamic quantities by considering a single Brownian particle that hops in underdamped medium along the potential $U(x) = U_s(x) + fx$, where $U_s(x)$ and f are the periodic potential and the external force, respectively.

For a single particle that is arranged to undergo a random walk, the dynamics of the particle is governed by the Langevin equation

$$m \frac{dv}{dt} = -\gamma \frac{dx}{dt} - \frac{dU(x)}{dx} + \sqrt{2k_B \gamma T(x)} \xi(t). \quad (1)$$

The Boltzmann constant k_B is assumed to be unity. The random noise $\xi(t)$ is assumed to be Gaussian white noise satisfying the relations $\langle \xi(t) \rangle = 0$ and $\langle \xi(t) \xi(t') \rangle = \delta(t - t')$. The viscous friction γ is assumed to be constant while the temperature $T(x)$ varies along the medium. For the underdamped Langevin case neither Ito nor Stratonovich interpretation is needed as discussed by Sancho *et al.* [27] and Jayannavar *et al.* [28].

For the overdamped case, the above Langevin equation can be written as

$$\gamma(x) \frac{dx}{dt} = \frac{-\partial U(x)}{\partial x} - \frac{(1 - \epsilon)}{\gamma(x)} \frac{\partial}{\partial x} [\gamma(x) T(x)] + \sqrt{2k_B \gamma(x) T(x)} \xi(t). \quad (2)$$

Here the Ito and Stratonovich interpretations correspond to the case where $\epsilon = 1$ and $\epsilon = 1/2$, respectively, while the case $\epsilon = 0$ is called the Hänggi postpoint or transform-form interpretation [27,29,30].

The Fokker-Plank equation for the underdamped case is given by

$$\frac{\partial P}{\partial t} = -\frac{\partial(vP)}{\partial x} - \frac{1}{m} \frac{\partial(U'(x)P)}{\partial v} + \frac{\gamma}{m} \frac{\partial(vP)}{\partial v} + \frac{\gamma T(x)}{m^2} \frac{\partial^2 P}{\partial v^2}, \quad (3)$$

where $P(x, v, t)$ is the probability of finding the particle at particular position, velocity, and time. The Gibbs entropy is given by

$$S(t) = - \int P(x, v, t) \ln P(x, v, t) dx dv. \quad (4)$$

The entropy production and dissipation rates can be derived via the approach stated in the work [7]. The derivative of S with time leads to

$$\frac{dS(t)}{dt} = -k_B \int \frac{\partial P(x, v, t)}{\partial t} \ln [P(x, v, t)] dx dv. \quad (5)$$

Equation (5) can be rewritten as

$$\frac{dS(t)}{dt} = \dot{e}_p - \dot{h}_d, \quad (6)$$

where $\dot{e}_p = \frac{de_p}{dt}$ and $\dot{h}_d = \frac{dh_d}{dt}$ are the entropy production and extraction rates.

In order to calculate \dot{h}_d , let us first find the heat dissipation rate \dot{H}_d via stochastic energetics that are discussed in the works in [31,32]. Accordingly the energy extraction rate can be written as

$$\begin{aligned}\dot{H}_d &= -\langle (-\gamma(x)\dot{x} + \sqrt{2k_B\gamma(x)T(x)}\cdot\dot{x}) \\ &= -\left\langle m\frac{v dv}{dt} + vU'(x) \right\rangle.\end{aligned}\quad (7)$$

Once the energy dissipation rate is obtained, based on our previous works [17–19], the entropy extraction rate \dot{h}_d then can be found as

$$\dot{h}_d = -\int \left(\frac{m\frac{v dv}{dt} + vU'(x)}{T(x)} \right) P dx dv. \quad (8)$$

At this point we want to stress that Eq. (8) is exact and does not depend on any boundary condition (as it can be seen in the next sections). Since $\frac{dS(t)}{dt}$ and \dot{h}_d are computable, the entropy production rate can be readily obtained as

$$\dot{e}_p = \frac{dS(t)}{dt} + \dot{h}_d. \quad (9)$$

In the high friction limit, Eq. (8) converges to

$$\dot{h}_d = -\int \left[J \frac{U'(x)}{T(x)} \right] dx, \quad (10)$$

where the probability current

$$J(x, t) = -\left[U'(x)P(x, t) + T(x)\frac{\partial P(x, t)}{\partial x} \right]. \quad (11)$$

At steady state $\frac{dS(t)}{dt} = 0$, which implies that $\dot{e}_p = \dot{h}_d > 0$. For the isothermal case, at stationary state (approaching equilibrium), $\dot{e}_p = \dot{h}_d = 0$.

Moreover, for the case where the probability distribution is either periodic or vanishes at the boundary, Tome *et al.* [26] derived the expressions for the entropy production and entropy extraction rates for the isothermal case. Following their approach, let us rewrite Eq. (3) as

$$\frac{\partial P}{\partial t} = k + \frac{\partial J'}{\partial v}, \quad (12)$$

where

$$k = v\frac{\partial P}{\partial x} + \frac{1}{m}(U')\frac{\partial P}{\partial v} \quad (13)$$

and

$$J' = -\frac{\gamma}{m}vP - \frac{T(x)}{m^2}\frac{\partial P}{\partial v}. \quad (14)$$

The expression k vanishes after imposing a boundary condition. After some algebra one gets

$$\dot{e}_p = -\int \frac{m^2 J'^2}{PT(x)\gamma} dx dv \quad (15)$$

and

$$\dot{h}_d = -\int \frac{mvJ'}{T(x)} dx dv, \quad (16)$$

respectively. In the next sections we show that indeed Eqs. (8) and (16) as well Eqs. (9) and (15) agree as long as a periodic boundary condition is imposed.

In general, since the expressions for $\dot{S}(t)$, $\dot{e}_p(t)$, and $\dot{h}_d(t)$ can be obtained at any time t , the analytic expressions for the change in entropy production, heat dissipation, and total entropy can be found analytically via

$$\begin{aligned}\Delta h_d(t) &= \int_0^t \dot{h}_d(t) dt, \\ \Delta e_p(t) &= \int_0^t \dot{e}_p(t) dt, \\ \Delta S(t) &= \int_0^t \dot{S}(t) dt,\end{aligned}\quad (17)$$

where $\Delta S(t) = \Delta e_p(t) - \Delta h_d(t)$.

Derivation for the free energy. The free energy dissipation rate $\dot{F}(t)$ can be expressed in terms of $\dot{E}_p(t)$ and $\dot{H}_d(t)$. $\dot{E}_p(t)$ and $\dot{H}_d(t)$ are the terms that are associated with $\dot{e}_p(t)$ and $\dot{h}_d(t)$. Let us now introduce $\dot{H}_d(t)$ for the model system we considered. The heat dissipation rate is either given by Eq. (7) (for any cases) or, if a periodic boundary condition is imposed, $\dot{H}_d(t)$ is given by

$$\dot{H}_d = -\int mvJ' dx dv. \quad (18)$$

Equation (18) is notably different from Eqs. (8) and (16), due to the term $T(x)$. On the other hand, the term \dot{E}_p is related to \dot{e}_p and it is given by

$$\dot{E}_p = -\int \frac{m^2 J'^2}{P\gamma} dx dv. \quad (19)$$

The new entropy balance equation

$$\frac{dS^T(t)}{dt} = \dot{E}_p - \dot{H}_d \quad (20)$$

is associated to Eq. (6) except the term $T(x)$. Once again, because the expressions for $\dot{S}^T(t)$, $\dot{E}_p(t)$, and $\dot{H}_d(t)$ can be obtained as a function of time t , the analytic expressions for the change related to the rate of entropy production, heat dissipation, and total entropy can be found analytically via

$$\begin{aligned}\Delta H_d(t) &= \int_0^t \dot{H}_d(t) dt, \\ \Delta E_p(t) &= \int_0^t \dot{E}_p(t) dt, \\ \Delta S(t)^T &= \int_0^t \dot{S}(t)^T dt,\end{aligned}\quad (21)$$

where $\Delta S(t)^T = \Delta E_p(t) - \Delta H_d(t)$.

On the other hand, the internal energy is given by

$$\dot{E}_{in} = \int [\dot{K} + vU'_s(x)]P(x, v, t) dv dx, \quad (22)$$

where $\dot{K} = m\frac{v dv}{dt}$ and U'_s denote the rate of kinetic and potential energy, respectively. For a Brownian particle that operates

due to the spatially varying temperature case, the total work done is then given by

$$\dot{W} = \int v f P(x, v, t) dv dx. \quad (23)$$

The first law of thermodynamics can be written as

$$\dot{E}_{\text{in}} = -\dot{H}_d(t) - \dot{W}. \quad (24)$$

The change in the internal energy reduces to $\Delta E_{\text{in}} = -\int_0^t [\dot{H}_d(t) + \dot{W}] dt$

As discussed in the work in [17–19], the rate of free energy is given by $\dot{F} = \dot{E} - T\dot{S}$ for the isothermal case and $\dot{F} = \dot{E} - \dot{S}^T$ for the nonisothermal case, where $\dot{S}^T = \dot{E}_p - \dot{H}_d$. Hence we write the free energy dissipation rate as

$$\dot{F} = \dot{E}_{\text{in}} - \dot{S}^T = \dot{E}_{\text{in}} - \dot{E}_p + \dot{H}_d. \quad (25)$$

The change in the free energy is given by

$$\Delta F(t) = -\int_0^t (\dot{W} + \dot{E}_p(t)) dt. \quad (26)$$

For the isothermal case, at quasistatic limit where the velocity approaches zero $v = 0$, $\dot{E}_p(t) = 0$, and $\dot{H}_d(t) = 0$ and far from quasistatic limit $E_p = \dot{H}_d > 0$, which is expected as the particle operates irreversibly.

III. ISOTHERMAL CASE

In this section we discuss the thermodynamic properties for a Brownian particle moving freely without any boundary condition in an underdamped medium under the influence of a force f in the absence of a potential U'_s . The general expression for the probability distribution $P(v, t)$ is calculated as

$$P(v, t) = \frac{e^{-\frac{m\left(\frac{-(1-e^{-\frac{\gamma t}{m}})t + v\right)^2}{2(1-e^{-\frac{2\gamma t}{m}})\gamma T}}}{\sqrt{2\pi}} \sqrt{\frac{m}{(1-e^{-\frac{2\gamma t}{m}})t}}. \quad (27)$$

The average velocity has the form

$$\langle v(t) \rangle = \left(\frac{1 - e^{-\frac{\gamma t}{m}}}{\gamma} \right) f. \quad (28)$$

At steady state (the long time limit), the velocity approaches $v = f/\gamma$ as expected.

A. Free particle diffusion

For a Brownian particle that moves in an underdamped medium without an external force, $f = 0$, next let us explore how the entropy production and extraction rates behave. From now on, whenever we plot any figures, we use the following dimensionless load $\bar{f} = fL_0/T_c$, $\bar{U} = U/T_c$, and temperature $\bar{\tau} = T(x)/T_c$, where T_c is the reference temperature. We also introduced dimensionless parameters $\bar{x} = x/L_0$, $\bar{v} = vm/\gamma L_0$, and $\bar{t} = t\gamma/m$. Hereafter the bar will be dropped. From now on all the figures will be plotted in terms of the dimensionless parameters.

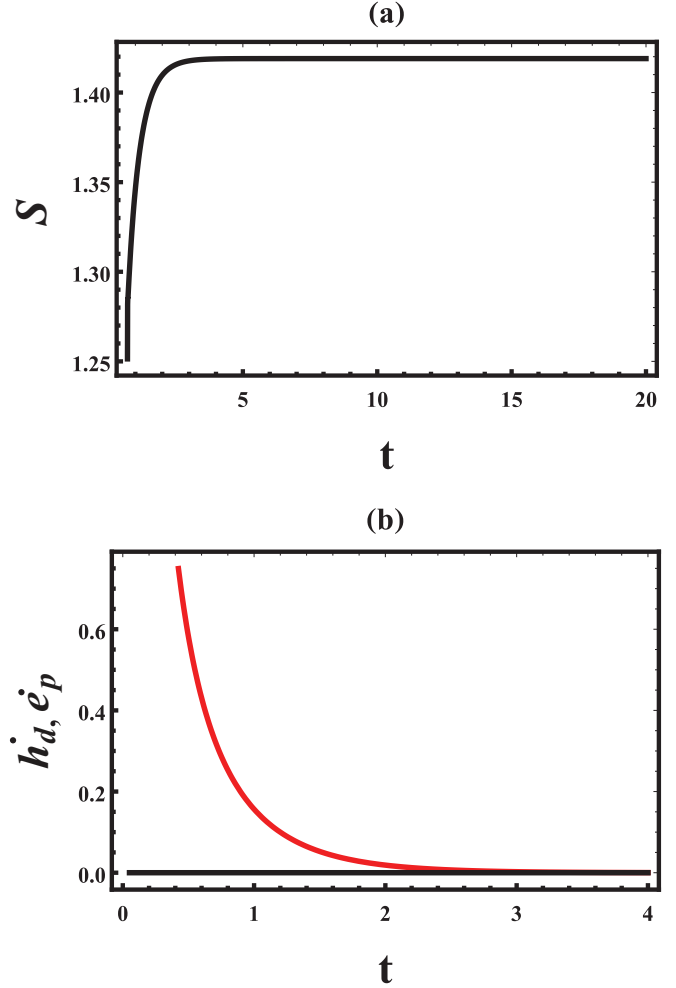


FIG. 1. (a) Entropy $S(t)$ as a function of t evaluated analytically by substituting Eq. (27) in Eq. (4). For the isothermal case where $\tau = 1$, $S(t)$ monotonously increases and saturates to a constant value as t further increases. (b) $\dot{e}_p(t)$ (black solid line) is analyzed analytically by substituting Eq. (27) in Eq. (9) while $\dot{h}_d(t)$ (red solid line) is calculated by plugging Eq. (27) in Eq. (10). The figure exhibits that $\dot{e}_p(t)$ decreases as time increases and, in the long time limit, it approaches its stationary value $\dot{e}_p(t) = \dot{h}_d(t) = 0$ as long as $\tau = 1$.

The expression for the entropy can be readily calculated by substituting Eq. (27) in Eq. (4). Figure 1 exhibits that the entropy $S(t)$ increases with time and saturates to a constant value which agrees with the results shown in the works [18,19]. On the other hand, the entropy production and extraction rates are explored via Eqs. (6), (8), and (9) (see Fig. 2). The plot $\dot{e}_p(t)$ (red solid line) and $\dot{h}_d(t)$ (black solid line) as a function of t for parameter choice $\tau = 1$ is depicted in Fig. 2. The figure exhibits that $\dot{e}_p(t)$ decreases as time increases and, in long time limit, it approaches its stationary value $\dot{e}_p(t) = 0$. On the other hand, $\dot{h}_d(t) = 0$ regardless of t . In the limit $t \rightarrow \infty$, $\frac{dS(t)}{dt} = 0$ since $\dot{e}_p(t) = \dot{h}_d(t) = 0$ in the long time limit. The above shown results can be explained intuitively on physical grounds. As one can note that for the isothermal case, in the long time limit the system reaches the stationary state. If the change in these parameters are taken at this particular state, then $\Delta h_d = 0$, $\Delta S = 0$, or $\Delta e_p = 0$. However, since

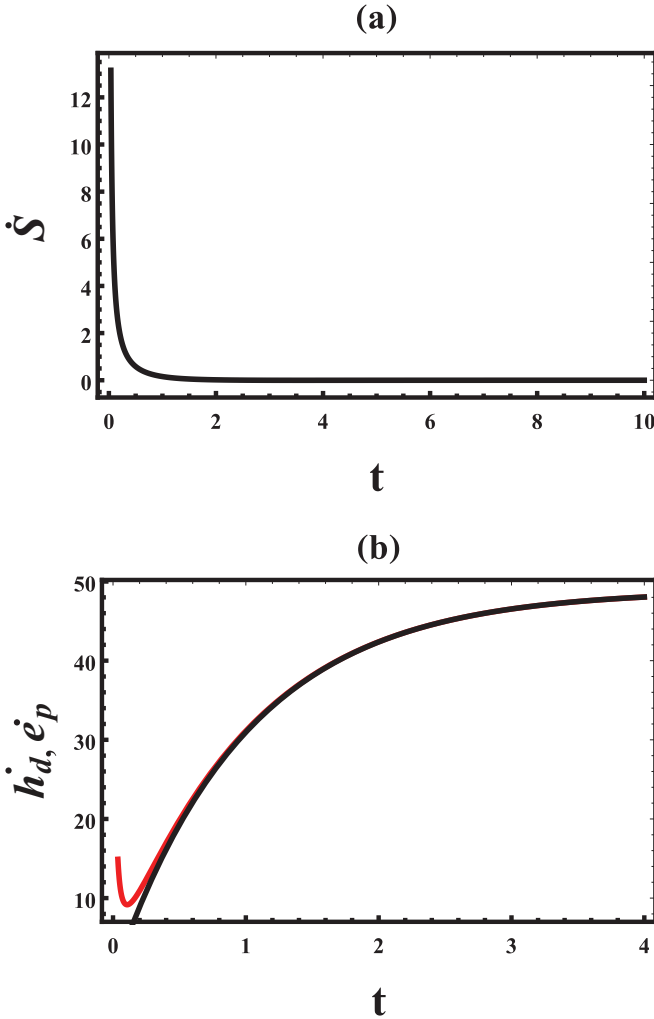


FIG. 2. (a) Entropy $\dot{S}(t)$ is determined analytically via Eq. (27) and Eq. (6). $S(t)$ monotonously increases and saturates to a constant value as t increases for fixed $\tau = 1$. At stationary state $\dot{S}(t) = 0$, which implies $\dot{e}_p(t) = \dot{h}_d(t)$. (b) $\dot{e}_p(t)$ (red solid line) as a function of t is plotted using Eq. (27) and Eq. (9), while $\dot{h}_d(t)$ (black solid line) as a function of t is evaluated by plugging Eq. (27) in Eq. (10). The figure exhibits that $\dot{e}_p(t)$ and $\dot{h}_d(t)$ increase as time increases and in the long time limit $\dot{e}_p(t) = \dot{h}_d(t) > 0$ as expected.

the system operates irreversibly at a finite time (far from the quasistatic limit), the second law of thermodynamics states that $\Delta S(t) > 0$. In reality, when the particle relaxes to its equilibrium state, it produces entropy and, once the motor starts operating, entropy will be accumulated in the system starting from $t = 0$ and, as time progresses, more entropy will be stored in the system even though some entropy is extracted out of the system. Hence if the change in these parameters is taken between $t = 0$ and any time t , always the inequality $\Delta h_d(t) = h_d(t) - h_d(0) > 0$, $\Delta S(t) = S(t) - S(0) > 0$, or $\Delta e_p(t) = e_p(t) - e_p(0) > 0$ holds true and as time progresses the change in these parameters increases. In fact, in small t regimes, $\dot{e}_p(t)$ becomes much larger than $\dot{h}_d(t)$, revealing that the entropy production is higher (than entropy extraction) in the first few periods of time. As time increases, more entropy will be extracted $\dot{h}_d(t) > \dot{e}_p$. Overall, since the

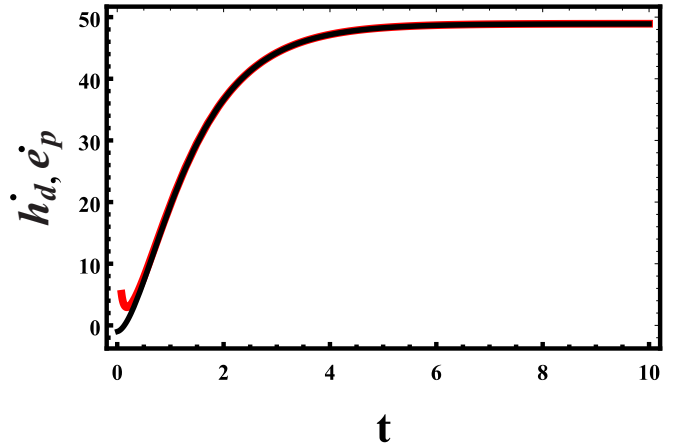


FIG. 3. Dependence of $\dot{e}_p(t)$ (black solid line) and $\dot{h}_d(t)$ (red solid line) on t is explored without imposing a periodic boundary condition. The results shown in Fig. 2 are identical to Fig. 3 except that Fig. 3 is plotted via Eqs. (6), (15), and (16), while in plotting Fig. 2, Eqs. (6), (8), and (9) are used.

system produces an enormous amount of entropy at the initial time, in latter time or any time t , $\Delta e_p(t) > \Delta h_d(t)$ and hence $\Delta S(t) > 0$.

B. Particle diffusion in the presence of force

In order to explore how the various thermodynamic relations behave when the system does work against the load f at a finite time, next we will explore the effect of the load f . In the presence of nonzero force, the particle diffuses under the influence of the external load. Exploiting Eqs. (6), (8), and (9), the dependence $\dot{S}(t)$, $\dot{e}_p(t)$, and $\dot{h}_d(t)$ on model parameters is explored. In Fig. 2(a), $\dot{S}(t)$ as a function of t is depicted for fixed values of $\tau = 1$ and $f = 1.0$. The figure clearly depicts that at small t , the entropy production rate is much greater than the entropy extraction rate. As time increases, the difference between $\dot{e}_p(t)$ and $\dot{h}_d(t)$ decreases and, in the limit $t \rightarrow \infty$, $S(t)$ saturates to zero showing that the system approaches its steady state. Figure 2(b) shows the plot $\dot{e}_p(t)$ as a function of t (red solid lines). In the same figure, the plot of $\dot{h}_d(t)$ versus t is shown (black solid line). The fact that $\dot{e}_p(t) > 0$ or $\dot{h}_d(t) > 0$ indicates that the system is out of equilibrium since the system does work at a finite time. Clearly at small t , $\dot{e}_p(t) > \dot{h}_d(t)$. As time progresses, $\dot{e}_p(t)$ and $\dot{h}_d(t)$ step up and, in long time limit, they approach their steady state values $\dot{h}_d(t) = \dot{e}_p(t) > 0$ revealing, in the presence of symmetry breaking fields such as external force, the system is driven out of equilibrium.

Even if no periodic boundary condition is imposed, the results shown in Fig. 2 can be also reproduced by employing Eqs. (6), (15), and (16). In fact Fig. 3 is identical to Fig. 2 except that Fig. 3 is plotted via Eqs. (6), (15), and (16) while, in plotting Fig. 2, Eqs. (6), (8), and (9) are used. Our analysis also indicates that the free energy dissipation rate \dot{F} is always less than zero $\dot{F} < 0$. As time steps up, it increases with time and approaches zero in the long time limit. All of the results shown in this work also agree with our previous results [17–19]. As before $\Delta h_d(t) = h_d(t) - h_d(t_0) > 0$, $\Delta S(t) = S(t) - S(t_0) > 0$, or $\Delta e_p(t) = e_p(t) - e_p(t_0) > 0$.

IV. NONISOTHERMAL CASE

A. Periodic boundary condition

Now let us consider an important model system where a colloidal particle undergoes a biased random walk in a spatially varying thermal arrangement in the presence of external load f with no potential. The load is also coupled with a heat bath that decreases from T_h at $x = 0$ to T_c at $x = L_0$ along the reaction coordinate in the manner

$$T(x) = \left\{ \frac{x(T_c - T_h)}{L_0} + T_h \right\}. \quad (29)$$

Here L_0 denotes the width of the ratchet potential. T_h and T_c denote the temperature of the hot and cold baths.

Solving Eq. (3) at steady state and imposing a periodic boundary condition, the general expression for the probability distribution is obtained as

$$P(x, v) = e^{-\frac{L_0 m (f - \gamma v)^2}{2\gamma^2 L_0 [L_0 T_h + (T_c - T_h)x]}} \sqrt{\frac{L_0 m}{2L_0 \pi T_h + 2\pi T_c x - 2\pi T_h x}}. \quad (30)$$

The average velocity is found to be

$$v = \frac{f}{\gamma}. \quad (31)$$

In the absence of force, the velocity approach zero.

Employing Eqs. (6), (8), and (9), the entropy production and extraction rates are calculated as

$$\dot{h}_d(t) = \dot{e}_p(t) = \frac{(2fL_0)^2 \ln[T_c/T_h]}{4\gamma L_0 (T_c - T_h)}. \quad (32)$$

We reproduce the above result (using Tome *et al.*'s [26] approach) via Eqs. (6), (15), and (16) as

$$\dot{h}_d(t) = \dot{e}_p(t) = \frac{(2fL_0)^2 \ln[T_c/T_h]}{4\gamma L_0 (T_c - T_h)}. \quad (33)$$

Surprisingly, in the limit where the load approaches the stall force, $\dot{h}_d(t) = \dot{e}_p(t) = 0$.

The rate of heat dissipation is calculated using Eq. (7) [or Eq. (18)] and it converges to

$$\dot{H}_d(t) = \dot{E}_p(t) = \frac{(fL_0)^2}{\gamma L_0}. \quad (34)$$

In the limit where the load approaches zero, $\dot{H}_d(t) = \dot{E}_p(t) = 0$, showing that at quasistatic limit the system is reversible. On the other hand, the rate of work done is given by

$$\dot{W}(t) = \dot{E}_p(t) = \frac{(fL_0)^2}{\gamma L_0}. \quad (35)$$

For isothermal case $T_h = T_c$ one gets $v = f/\gamma$, $\dot{h}_d(t) = \dot{e}_p(t) = f^2 L_0 / \gamma T_c$, and $\dot{H}_d(t) = \dot{E}_p(t) = f^2 L_0 / \gamma$.

All of the results shown in this section are justified via numerical simulations by integrating the Langevin equation (1) (employing Brownian dynamics simulation). In the simulation, a Brownian particle is initially situated in one of the potential wells. Then the trajectories for the particle are simulated by considering different time steps Δt and time length t_{max} . In order to ensure the numerical accuracy 10^9 ensemble averages have been obtained. Figure 4 depicts the

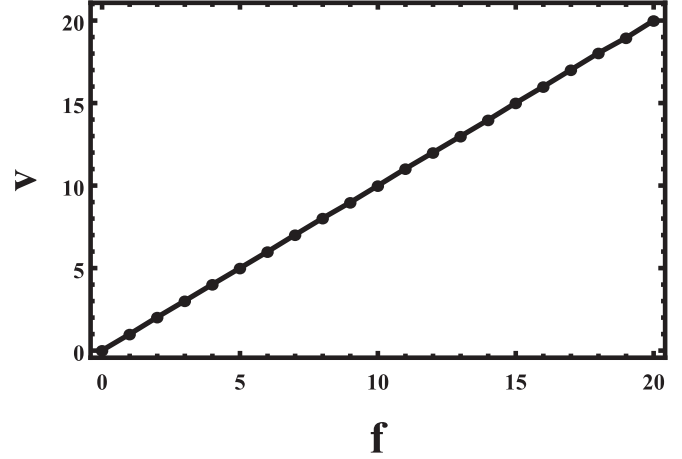


FIG. 4. Velocity v as a function of load f . The dotted line is plotted via Brownian dynamic simulation, while the solid line is plotted using the analytic Eq. (31). The figure depicts that, as the strength of force steps up, the velocity of the particle increases.

plot v as a function of load f . The dotted line is plotted via Brownian dynamic simulation while the solid line is plotted using the analytic Eq. (31). The figure shows the velocity steps up linearly with the load f . This is feasible since the unbiased random walk is due to the applied load f . The plot $\dot{e}_p(t)$ and $\dot{h}_d(t)$ as a function of f is depicted in Fig. 5(a) for parameter choice $\tau = 2$. The figures show that $\dot{e}_p(t)$ and $\dot{h}_d(t)$ have a nonlinear dependence on the load. As the load steps up, $\dot{e}_p(t)$ and $\dot{h}_d(t)$ increase, showing the entropy production and extraction rates intensify with load.

In order to investigate the effect of the temperature difference between the hot and cold baths, next we study the system as a function of the rescaled temperature $\tau = T_h/T_c$. Figure 5(b) exhibits the plot $\dot{e}_p(t)$ and $\dot{h}_d(t)$ as a function of τ for fixed $f = 2$. The figure depicts that $\dot{e}_p(t)$ and $\dot{h}_d(t)$ decrease as the temperature increases.

B. Nonisothermal case without boundary condition

All the discussed thermodynamic quantities are quite sensitive to the choice of the boundary condition. For instance, when no boundary condition is imposed, we find the velocity for the underdamped case as

$$v = \frac{2fL_0 + (T_c - T_h)}{2\gamma L_0}, \quad (36)$$

showing the particle stalls when

$$f_s = \frac{(T_h - T_c)}{2\gamma L_0}. \quad (37)$$

When $f < f_s$, the particle velocity $v > 0$ and, if $f > f_s$, the particle velocity $v < 0$. At stall force $f = f_s$, $v = 0$. The entropy production and extraction rates are given as

$$\dot{h}_d(t) = \dot{e}_p(t) = \frac{(2fL_0 + T_c - T_h)^2 \ln[T_c/T_h]}{4\gamma L_0 (T_c - T_h)}, \quad (38)$$

while

$$\dot{H}_d(t) = \dot{E}_p(t) = \frac{(2fL_0 + T_c - T_h)^2}{4\gamma L_0}. \quad (39)$$

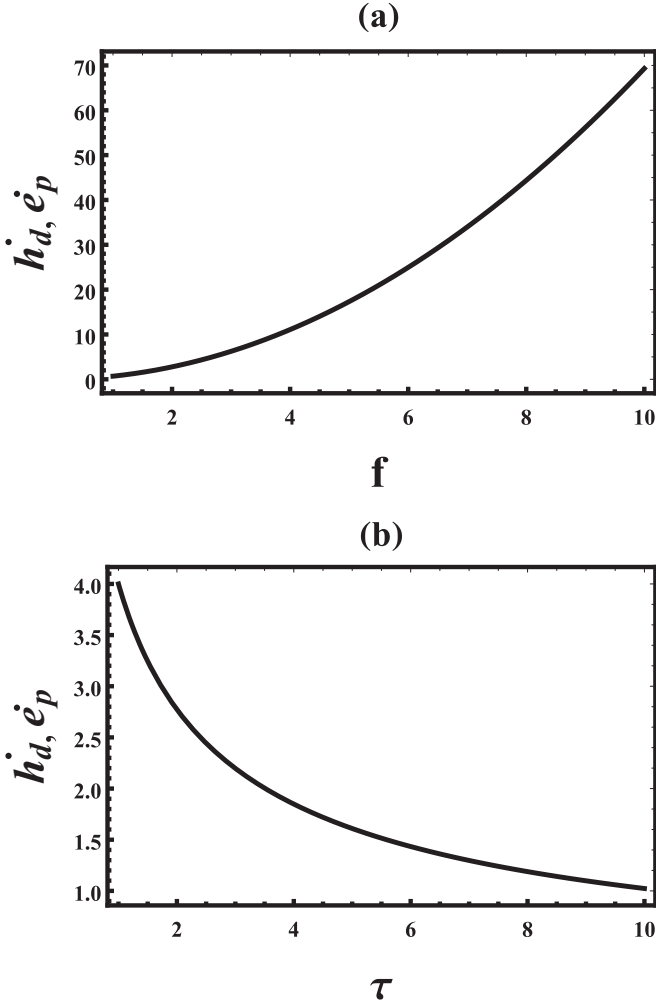


FIG. 5. (a) Dependence of $\dot{e}_p(t)$ and $\dot{h}_d(t)$ on the load f is evaluated analytically via Eq. (32) or Eq. (33). (b) The plot $\dot{e}_p(t)$ and $\dot{h}_d(t)$ as a function of τ for parameter choice $f = 2$.

Exploiting Eq. (38), one can see that, in the limit $f \rightarrow f_s$, $\dot{h}_d(t) \rightarrow 0$ and $\dot{e}_p(t) \rightarrow 0$. All of these results indicate that, in the absence of boundary conditions, most of the thermodynamic quantities have a functional dependence on $\Delta T = T_h - T_c$, which agrees with the work by Matsuo *et al.* [33].

V. BROWNIAN PARTICLE WALKING IN A RATCHET POTENTIAL WHERE THE POTENTIAL IS COUPLED WITH A SPATIALLY VARYING TEMPERATURE

In this section, let us consider a Brownian particle that moves along the potential $U(x) = U_s(x) + fx$, where f and $U_s(x)$ denote the load and ratchet potential, respectively. (See Fig. 6.) The ratchet potential $U_s(x)$

$$U_s(x) = \begin{cases} 2U_0[\frac{x}{L_0}], & \text{if } 0 < x \leq L_0/2, \\ 2U_0[\frac{-x}{L_0} + 1], & \text{if } L_0/2 < x \leq L_0 \end{cases} \quad (40)$$

is coupled with a heat bath that decreases from T_h at $x = 0$ to T_c at $x = L_0$ along the reaction coordinate in the manner

$$T(x) = \left\{ \frac{x(T_c - T_h)}{L_0} + T_h \right\}. \quad (41)$$

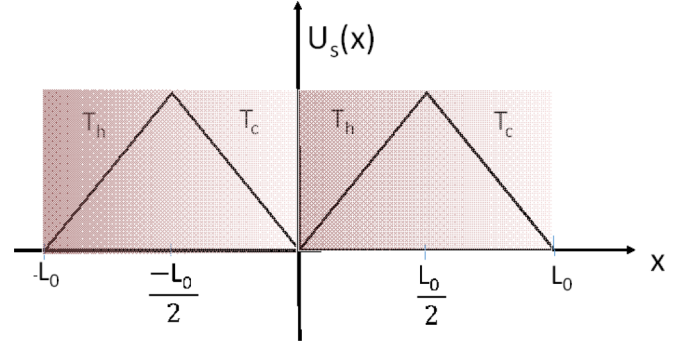


FIG. 6. Schematic diagram for a Brownian particle in a piecewise linear potential in the absence of external load. Due to the thermal background kicks, the particle ultimately attains a steady state current (velocity) as long as a distinct temperature difference between the hot and the cold reservoirs is retained.

Here U_0 denotes the barrier height. The ratchet potential has a potential maxima at $x = L_0/2$ and potential minima at $x = 0$ and $x = L_0$. The potential profile repeats itself such that $U_s(x + L_0) = U_s(x)$. Next let us consider the underdamped case.

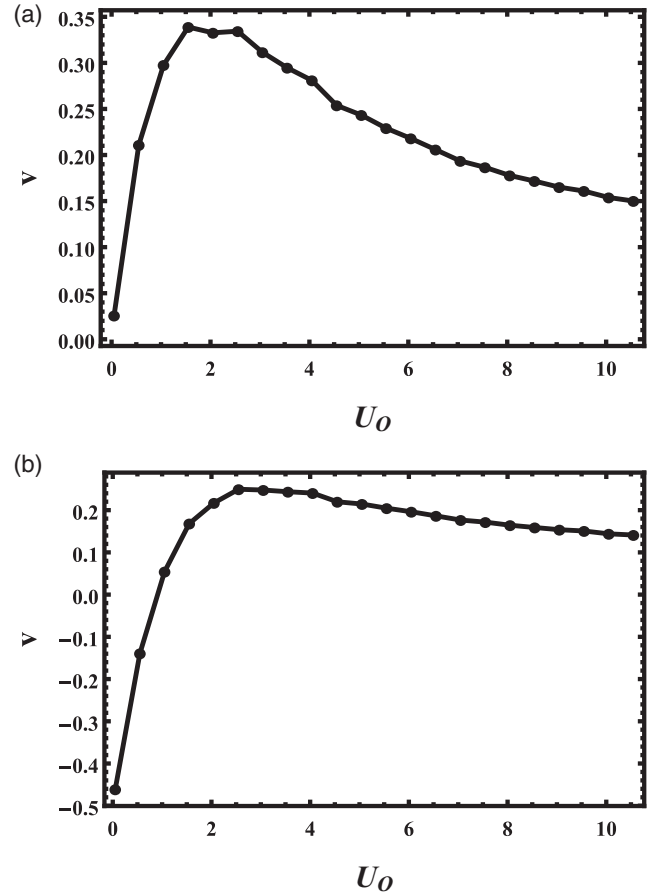


FIG. 7. (a) v versus U_0 for fixed $\tau = 2$, $f = 0.0$, $m = 1$, and $\gamma = 1$. (b) v as a function of U_0 for fixed $\tau = 2$ and $f = 0.5$. In both figures, the velocity is determined via numerical simulations by integrating Eq. (1).

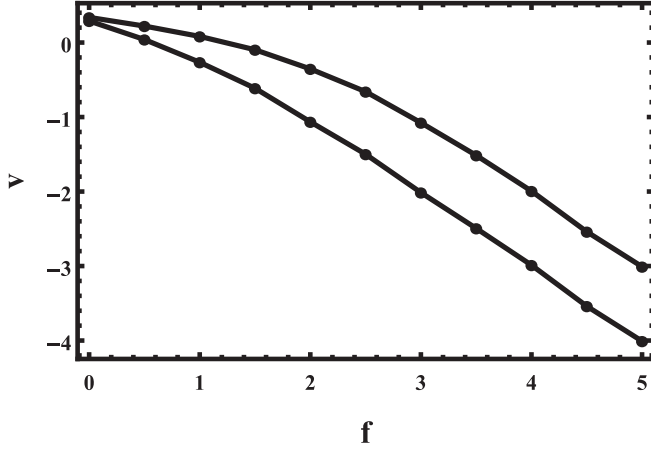


FIG. 8. Numerical simulation result depicts that the velocity monotonously decreases as the load increases. At stall force, the particle velocity is zero and, as the load further increases, the particle velocity gets reversed. In the figure, the parameters are fixed as $\tau = 2$, $U_0 = 2.0$ (top), and $U_0 = 1.0$ (bottom).

A. Underdamped case

Let us now explore the dependence of thermodynamic quantities via numerical simulations by integrating Eq. (1). As one can note, a Brownian motor that is exposed to operate in such a model system exhibits a unidirectional motion even in the absence of a load as long as the height of potential U_0 is nonzero. This shows that U_0 is an important model parameter that dictates the operation of the motor and next we explore how the different thermodynamic relations behave as U_0 varies.

In Fig. 7(a), the plot of v as a function of U_0 is depicted for fixed $\tau = 2$, $f = 0.0$, $m = 1$, and $\gamma = 1$. The figure shows that the velocity peaks at a certain U_0 . On the other hand, the plot of v as a function of U_0 is shown in Fig. 7(b) for fixed $\tau = 2$, $f = 0.5$, $m = 1$, and $\gamma = 1$. The figure shows that the velocity is negative below a certain U_0 . As U_0 steps up the velocity steps up and attains an optimum value. The velocity decreases monotonously when the load steps as shown in Fig. 8. At stall force the velocity becomes zero. Further increases in the load lead to a current reversal. The plot $\dot{e}_p(t)$ and $\dot{h}_d(t)$ as a function of U_0 for parameter choice $f = 2$ is determined via simulations as shown in Fig. 9. The main result indicates that, in the regions where the motor moves fast, the entropy production and extraction rates are significantly high.

B. Overdamped case

In the high friction limit, as discussed before, the dynamics of the particle is governed by the Langevin equation

$$\gamma(x) \frac{dx}{dt} = -\frac{\partial[U(x) + \frac{T(x)}{2}]}{\partial x} + \sqrt{2k_B\gamma(x)T(x)}\xi(t). \quad (42)$$

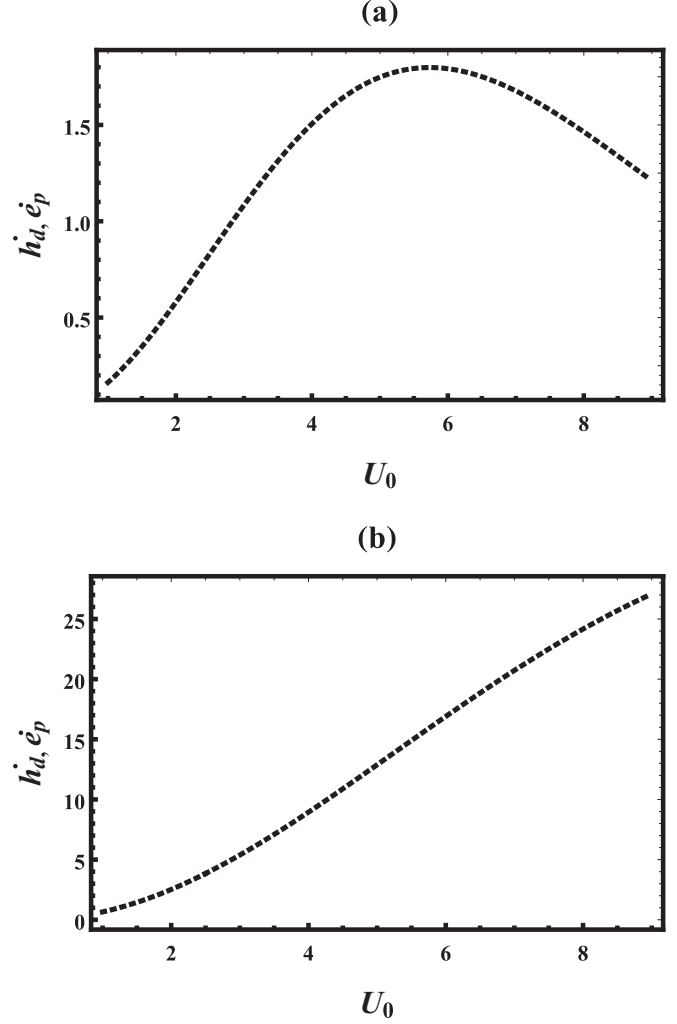


FIG. 9. (a) Plot $\dot{e}_p(t)$ and $\dot{h}_d(t)$ as a function of U_0 for parameter choice $\tau = 12$ and $f = 0.5$. (b) The plot $\dot{e}_p(t)$ and $\dot{h}_d(t)$ as a function of U_0 for parameter choice $f = 2.0$ (solid line) and $\tau = 2.0$.

Assuming γ to be unity, the corresponding Fokker Planck equation is given by

$$\frac{\partial P(x, t)}{\partial t} = \frac{\partial}{\partial x} \left[U'(x)P(x, t) + \frac{T'(x)}{2}P(x, t) + T(x) \frac{\partial}{\partial x} P(x, t) \right], \quad (43)$$

where $P(x, t)$ is the probability density of finding the particle at position x at time t , $U'(x) = \frac{d}{dx}U$. The current is given by

$$J(x, t) = - \left[U'(x)P(x, t) + \frac{T'(x)}{2}P(x, t) + T(x) \frac{\partial P(x, t)}{\partial x} \right]. \quad (44)$$

In long time limit, the expression for the constant current, J , is given in Appendix. The change in entropy is given as [19]

$$\begin{aligned} \frac{dS(t)}{dt} &= \dot{e}_p - \dot{h}_d \\ &= \int \frac{J^2}{P(x, t)T(x)} + J \frac{U'(x)}{T(x)} + J \frac{T'(x)}{2T(x)} dx, \quad (45) \end{aligned}$$

where the entropy production rate \dot{e}_p and dissipation rate \dot{h}_d are given as

$$\dot{e}_p = \int \frac{J^2}{P(x,t)T(x)} dx \quad (46)$$

and

$$\dot{h}_d = \int \left(J \frac{U'(x)}{T(x)} + \frac{JT'(x)}{2T(x)} \right) dx, \quad (47)$$

respectively. Here, unlike the isothermal case, we have the additional term $J \frac{T'(x)}{2T(x)} dx$. At steady state $\frac{dS(t)}{dt} = 0$, which implies that $\dot{e}_p = \dot{h}_d > 0$. At stationary state (approaching equilibrium), $J = 0$, since a detailed balance condition is preserved. Hence $\dot{e}_p = \dot{h}_d = 0$.

In order to relate the free energy dissipation rate with $\dot{E}_p(t)$ and $\dot{H}_d(t)$ let us now introduce $\dot{H}_d(t)$ for the model system we considered. The heat dissipation rate is given by

$$\dot{H}_d = \int \left(JU'(x) + \frac{JT'(x)}{2} \right) dx. \quad (48)$$

\dot{E}_p is the term related to \dot{e}_p and it is given by

$$\dot{E}_p = \int \left(\frac{J^2}{P(x,t)} \right) dx. \quad (49)$$

We have now a new entropy balance equation

$$\begin{aligned} \frac{dS(t)^T}{dt} &= \dot{E}_p - \dot{H}_d \\ &= \int \left(\frac{J^2}{P(x,t)} + JU'(x) + JT'(x) \right). \end{aligned} \quad (50)$$

Since the analytic expressions for $J(x,t)$ and $P(x,t)$ are given in Appendix, all of the above expressions are exact but lengthy.

If one considers a periodic boundary condition at steady state in the absence of ratchet potential $U_0 = 0$, the results obtained quantitatively agree with the underdamped case (Sec. IV) and one gets

$$\dot{h}_d(t) = \dot{e}_p(t) = \frac{(2fL_0)^2 \ln[T_c/T_h]}{4L_0(T_c - T_h)} \quad (51)$$

and

$$\dot{H}_d(t) = \dot{E}_p(t) = \frac{(fL_0)^2}{L_0}. \quad (52)$$

The steady state current is zero at stall load

$$f_s = \frac{2U_0}{L} \frac{\ln \left[\frac{4\tau}{(1+\tau)^2} \right]}{\ln \left[\frac{1}{\tau} \right]}, \quad (53)$$

which implies the particle velocity $v > 0$ when $f < f_s$ and at stall force $v = 0$. When $f > f_s$, $v < 0$. In the quasistatic limit $v \rightarrow 0$ ($J \rightarrow 0$), the system is reversible.

On the contrary, in the absence of any boundary condition, the calculated thermodynamic quantities are quantitatively the same as the result shown in Sec. IV B. For instance, in the absence of potential, the velocity can be calculated as $v = JL$. Alternatively, we can also find v by taking the time average of

Eq. (42) as

$$\begin{aligned} \gamma v &= \left\langle \frac{\partial(fx + \frac{T(x)}{2})}{\partial x} + \sqrt{2k_B\gamma(x)T(x)}\xi(t) \right\rangle, \\ \gamma v &= f + \frac{(T_h - T_c)}{2L_0}, \\ v &= \frac{2fL_0 + (T_c - T_h)}{2\gamma L_0}. \end{aligned} \quad (54)$$

Equation (54) is the same as Eq. (36). At this point, we want to stress that, at steady state, most of the derived physical quantities are similar both quantitatively and qualitatively whether the particle is in underdamped or overdamped medium.

Derivation for the free energy. Next assuming a periodic boundary condition where the term $T'(x)$ vanishes, let us further explore the model system. The expressions for the work done by the Brownian particle as well as the amount of heat taken from the hot bath and the amount of heat given to the cold reservoir can be derived in terms of the stochastic energetics discussed in the works in [31,32]. The heat taken from any heat bath can be evaluated via [31,32] $\dot{Q} = \langle (-\gamma(x)\dot{x} + \sqrt{2k_B\gamma(x)T(x)}) \cdot \dot{x} \rangle$, while the work done by the Brownian particle against the load is given by $\dot{W} = \langle f\dot{x} \rangle$. We can also find the expression for the input heat Q_{in}^s and W^s as

$$\begin{aligned} \dot{Q}_{in} &= \int_0^{L_0/2} (-\gamma(x)\dot{x} + \sqrt{2k_B\gamma(x)T(x)})J dx \\ &= \int_0^{L_0/2} \left[\left(\frac{2U_0}{L_0} \right) + f \right] J dx \\ &= U_0J + \frac{fL_0J}{2}. \end{aligned} \quad (55)$$

Here the integral is evaluated in the interval of $(0, L_0/2)$ since the particle has to get a minimal amount of heat input from the heat bath located in the left side of the ratchet potential to surmount the potential barrier. The work done is also given by

$$\dot{W} = \int_0^{L_0} f dx = fL_0J. \quad (56)$$

The first law of thermodynamics states that $Q_{in}^s - Q_{out}^s = W^s$, where Q_{out}^s is the heat given to the colder heat bath. Thus

$$\dot{Q}_{out} = \dot{Q}_{in} - \dot{W} = U_0J - \frac{fL_0J}{2}. \quad (57)$$

The second law of thermodynamics can be rewritten in terms of the housekeeping heat and excess heat. For the model system we consider, when the particle undergoes a cyclic motion, at least it has to get fLJ amount of energy rate from the hot reservoir in order to keep the system at steady state. Hence fLJ is equivalent to the housekeeping heat Q_{hk} and we can rewrite Eq. (25) as

$$\dot{F}(t) + \dot{E}_p(t) = \dot{E}_{in}(t) + \dot{H}_d(t) = -fLJ = -\dot{Q}_{hk}, \quad (58)$$

while the expression for the excess heat \dot{Q}_{ex} is given by

$$Q_{ex} = \dot{H}_d - \dot{Q}_{hk}. \quad (59)$$

For the isothermal case, we can rewrite the second law of thermodynamics as

$$\dot{S}^T(t) = \dot{E}_p - \dot{H}_d = -\dot{F} - \dot{Q}_{ex} \quad (60)$$

and

$$\dot{F} = \dot{Q}_{hk} - \dot{E}_p. \quad (61)$$

At this point we want to stress that such kind of Brownian motor is inherently irreversible. This can be more appreciated by calculating the efficiency of the engine. The efficiency is given as

$$\eta = W/Q_{in}. \quad (62)$$

In the quasistatic limit ($J \rightarrow 0$), we find

$$\eta = 1 - \frac{\ln\left[\frac{1+\tau}{2\tau}\right]}{\ln\left[\frac{2}{\tau+1}\right]}, \quad (63)$$

which is approximately equal to the efficiency of the endoreversible heat engine η_{CA}

$$\eta_{CA} = 1 - \sqrt{1/\tau}, \quad (64)$$

as long as the temperature difference between the hot and the cold reservoirs is not large. In order to appreciate this let us Taylor expand Eqs. (63) and (64) around $\tau = 1$ and after some algebra one gets

$$\begin{aligned} \eta &= \eta_{CA} = \frac{\tau - 1}{2} - \frac{3}{8}(\tau - 1)^2 + \dots \\ &= \frac{\eta_{CAR}}{2} + \frac{\eta_{CAR}^2}{8} + \frac{\eta_{CAR}^3}{96} + \dots, \end{aligned} \quad (65)$$

which exhibits that both efficiencies are equivalent in this regime. Here η_{CAR} is the Carnot efficiency $\eta_{CAR} = 1 - 1/\tau$.

Next we study how the rate of entropy production $\dot{e}_p(t)$ and the rate of entropy extraction $\dot{h}_d(t)$ behave. The plot of $\dot{e}_p(t)$ and $\dot{h}_d(t)$ as a function of f is depicted in Fig. 10(a) for fixed values of $U_0 = 2.0$ and $\tau = 12.0$. Once again the figure indicates that the entropy production and extraction rates take nonzero values as long as the system is driven out of equilibrium. At stall force (zero velocity), $\dot{e}_p(t) = \dot{h}_d(t) = 0$, which implies that at the stall force the system is reversible.

The plot $\dot{e}_p(t)$ and $\dot{h}_d(t)$ as a function of τ is depicted in Fig. 10(b) for parameter choice $f = 2.0$ and $U_0 = 2.0$. The figure indicates, as τ steps up, both the entropy production and extraction rates decrease but still $\dot{e}_p(t) > 0$ and $\dot{h}_d(t) > 0$ and, at a certain τ , $\dot{e}_p(t) = \dot{h}_d(t) = 0$. This is because at this particular rescaled temperature τ , the particle stalls. As τ further increases, the entropy production and extraction rates increase.

VI. FLUCTUATION THEOREM

As discussed in our previous work [19], the phase space trajectory is defined as $x(t) = x_0, x_1, x_\tau$, where x_s signifies the phase space at $t = t_s$. Whenever the sequence of noise terms for the total time of observation $\xi = \xi_0, \xi_1, \xi_{s_1}$ is available, from the knowledge of the initial point x_0 , $x(t)$ will be then determined. The probability of obtaining the sequence ξ is given as

$$P[\xi(t)] \propto e^{[-\frac{1}{2} \int_0^\tau \xi^2(t) dt]}. \quad (66)$$

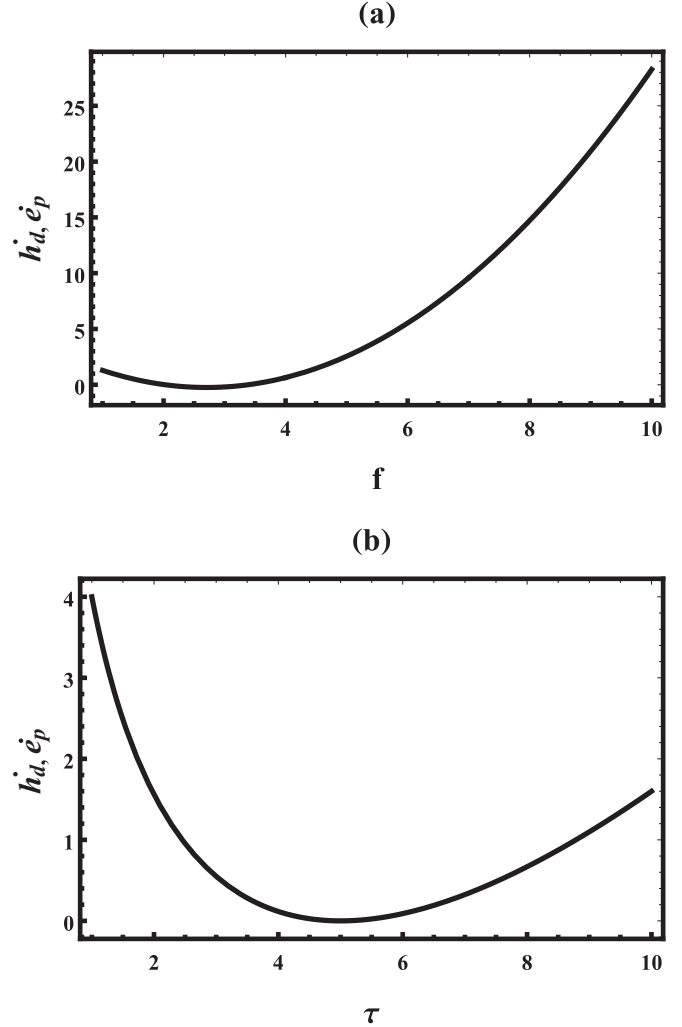


FIG. 10. (a) Dependence of $\dot{e}_p(t)$ and $\dot{h}_d(t)$ on the load f and τ is examined analytically using Eqs. (46) and (47). In (a), we fix $\tau = 12$ and $U_0 = 2$. (b) The plot $\dot{e}_p(t)$ and $\dot{h}_d(t)$ as a function of τ for parameter choice $f = 2.0$ and $U_0 = 2.0$.

Since the Jacobian for reverse and forward process is the same, $P[x(t)|x_0]$ is proportional:

$$\begin{aligned} P[x(t)|x_0] &\propto e^{[-\frac{1}{2} \int_0^\tau \xi^2(t) dt]} \\ &\propto e^{[-\frac{1}{4} \int_0^\tau dt \frac{(m \frac{dv}{dt} + U + \frac{T}{2} + \dot{x})^2}{T}]} \end{aligned} \quad (67)$$

Because the Jacobian for reverse and forward process is the same, $P[x(t)|x_0]$ is proportional, and one gets

$$\begin{aligned} \frac{P[x(t)|x_0]}{P[\tilde{x}(t)|\tilde{x}_0]} &= \frac{e^{[-\frac{1}{4} \int_0^\tau dt \frac{(m \frac{dv}{dt} + U + \frac{T}{2} + \dot{x})^2}{T}]}{e^{[-\frac{1}{4} \int_0^\tau dt \frac{(m \frac{dv}{dt} + U + \frac{T}{2} - \dot{x})^2}{T}]} \\ &= e^{[-\int_0^\tau dt \frac{(m \frac{dv}{dt} + U + \frac{T}{2}) \dot{x}}{T}]} \\ &= e^{-\Delta h_d^*(t)}. \end{aligned} \quad (68)$$

Here $h_d^*(t)$ is related with Eq. (8). This implies $\ln\left[\frac{P[x(t)|x_0]}{P[\tilde{x}(t)|\tilde{x}_0]}\right] = -\Delta h_d^*(t)$. For the Markov chain, since $P[x(t)|x(0)] = \frac{P[x(t), x(0)]}{P[x(0)]}$, $\ln\left[\frac{P[x(t)|x_0]}{P[\tilde{x}(t)|\tilde{x}_0]}\right] = \ln\left[\frac{P[x(t)]}{P[\tilde{x}(t)]}\right] - \ln\left[\frac{P[x_0]}{P[\tilde{x}_0]}\right] = -\Delta h_d^*(t)$.

This also implies that $\ln\left[\frac{P[x(t)]}{P[x_0]}\right] = -\Delta e_h^*(t)$ and $\ln\left[\frac{P[x_0]}{P[x(t)]}\right] = -\Delta s^*(t)$. Clearly the integral fluctuation relation

$$\langle e^{-\Delta e_h^*(t)} \rangle = 1. \quad (69)$$

VII. SUMMARY AND CONCLUSION

In this work, via Langevin equation and using Boltzmann-Gibbs nonequilibrium entropy, the general expressions for the free energy, entropy production rate \dot{e}_p , and entropy extraction rate \dot{h}_d are derived in terms of velocity and probability distribution considering the underdamped Brownian motion case. After extending the results obtained by Tome *et al.* to the spatially varying temperature case, we further analyze our model systems. We show that the entropy production rate \dot{e}_p increases in time and at steady state (in the presence of load), $\dot{e}_p = \dot{h}_d > 0$. At stationary state (in the absence of load), $\dot{e}_p = \dot{h}_d = 0$. When the particle hops on nonisothermal medium where the medium temperature is linearly decreasing (in the presence of load), the exact analytic results exhibit that the velocity approach is zero only when the load approaches zero. We show that the approximation performed based on Tome *et al.* and our general analytic expression agrees quantitatively. The analytic results also justified via numerical simulations.

Furthermore, we discuss the nonequilibrium thermodynamic features of a Brownian particle that hops in a ratchet potential where the potential is coupled with a spatially varying temperature. It is shown that the operational regime of such Brownian heat engine is dictated by the magnitude of the external load f . The steady state current or equivalently the velocity of the engine is positive when f is smaller and the engine acts as a heat engine. In this regime $\dot{e}_p = \dot{h}_d > 0$. When f increases, the velocity of the particle decreases and, at stall force, we find that $\dot{e}_p = \dot{h}_d = 0$, showing that the system is reversible at this particular choice of parameter. For large load, the current is negative and the engine acts as a refrigerator. In this region $\dot{e}_p = \dot{h}_d < 0$.

In conclusion, several thermodynamic relations are derived for a Brownian particle moving in underdamped medium by considering different relevant model systems. The present theoretical work not only serves as an important tool to investigate thermodynamic features of the particle but also advances the physics of nonequilibrium thermodynamics.

ACKNOWLEDGMENT

I would like to thank Blaynesh Bezabih and Mulu Zebene for their constant encouragement.

APPENDIX: DERIVATION OF STEADY STATE CURRENT

For a Brownian particle that moves along the ratchet potential [Eq. (40)] with load $U_s(x + L_0) = U_s(x)$, in the high friction limit, the dynamics of the particle is governed by the Langevin equation

$$\gamma(x) \frac{dx}{dt} = -\frac{\partial[U(x) + \frac{T(x)}{2}]}{\partial x} + \sqrt{2k_B\gamma(x)T(x)}\xi(t), \quad (A1)$$

where $T(x)$ is given in Eq. (41). The corresponding Fokker-Planck equation is given by

$$\frac{\partial P(x, t)}{\partial t} = \frac{\partial}{\partial x} \left[U'(x)P(x, t) + \frac{T'(x)}{2}P(x, t) + T(x) \frac{\partial}{\partial x} P(x, t) \right], \quad (A2)$$

where $P(x, t)$ is the probability density of finding the particle at position x at time t , $U'(x) = \frac{d}{dx}U$. The current is given by

$$J(x, t) = -\left[U'(x)P(x, t) + \frac{T'(x)}{2}P(x, t) + T(x) \frac{\partial P(x, t)}{\partial x} \right]. \quad (A3)$$

The general expression for the steady state current J for any periodic potential with or without load is reported in the works in [34]. Following the same approach, we find the steady state current J as

$$J = \frac{-F}{G_1 G_2 + H F}, \quad (A4)$$

where the expressions for F , G_1 , G_2 , and H are given as

$$F = -1 + e^{-\frac{2U_2 \ln \frac{1+\tau}{1-\tau} + 2U_1 \ln \frac{1+\tau}{1-\tau}}{\tau}}, \quad (A5)$$

$$G_1 = \frac{1 - 4 \frac{U_1}{1-\tau} \left(\frac{\tau}{1+\tau}\right)^{\frac{2U_1}{1-\tau}}}{2U_1} + \frac{2^{-1+\frac{2U_1}{1-\tau}} \left(\frac{1+\tau}{\tau}\right)^{-\frac{2U_1}{1-\tau}} \left[-1 + 4 \frac{U_2}{1-\tau} \left(\frac{1}{1+\tau}\right)^{\frac{2U_2}{1-\tau}} \right]}{U_2}, \quad (A6)$$

$$G_2 = \frac{1}{2} \left(\frac{2\tau}{-1 + \tau - 2U_1} - \frac{4 \frac{U_1}{1-\tau} \left(1 + \frac{1}{\tau}\right)^{-\frac{2U_1}{1-\tau}} (1 + \tau)}{-1 + \tau - 2U_1} \right) + \frac{1}{2} \left(\frac{4 \frac{U_1}{1-\tau} \left(1 + \frac{1}{\tau}\right)^{-\frac{2U_1}{1-\tau}} [1 + \tau - 2^{1+\frac{2U_2}{1-\tau}} \left(\frac{1}{1+\tau}\right)^{\frac{2U_2}{1-\tau}}]}{-1 + \tau + 2U_2} \right), \quad (A7)$$

$$H = T_1 + T_2(T_3 + T_4 + T_5), \quad (A8)$$

$$T_1 = \frac{\tau \left[-1 + 4 \frac{U_1}{1-\tau} \left(\frac{\tau}{1+\tau}\right)^{\frac{2U_1}{1-\tau}} \right] + U_1}{2U_1(1 - \tau + 2U_1)}, \quad (A9)$$

$$T_2 = 2^{-2+\frac{2(U_1+U_2)}{1-\tau}} \left(\frac{1 + \tau}{\tau}\right)^{-\frac{2U_1}{1-\tau}}, \quad (A10)$$

$$T_3 = \frac{2^{\frac{1-\tau-2(U_1+U_2)}{1-\tau}} \left(\frac{1+\tau}{\tau}\right)^{\frac{2U_1}{1-\tau}}}{1 - \tau - 2U_2} + \frac{2\tau \left[-4^{-\frac{U_2}{1-\tau}} + \left(\frac{1}{1+\tau}\right)^{\frac{2U_2}{1-\tau}} \right]}{(-1 + \tau - 2U_1)U_2}, \quad (A11)$$

$$T_4 = \frac{2^{-\frac{2U_1}{1-\tau}} (1 + \tau) \left(\frac{1+\tau}{\tau}\right)^{\frac{2U_1}{1-\tau}} \left[-2^{-\frac{2U_2}{1-\tau}} + \left(\frac{1}{1+\tau}\right)^{\frac{2U_2}{1-\tau}} \right]}{(1 - \tau + 2U_1)U_2}, \quad (A12)$$

$$T_5 = -\frac{2^{-\frac{2U_1}{1-\tau}} (1 + \tau) \left(\frac{1+\tau}{\tau}\right)^{\frac{2U_1}{1-\tau}} \left[-2^{-\frac{2U_2}{1-\tau}} + \left(\frac{1}{1+\tau}\right)^{\frac{2U_2}{1-\tau}} \right]}{(1 - \tau - 2U_2)U_2}. \quad (A13)$$

Here $U_1 = U_0 + f/2$ and $U_2 = U_0 - f/2$. The expression for the velocity is then given by $V = LJ$.

- [1] H. Ge and H. Qian, *Phys. Rev. E* **81**, 051133 (2010).
- [2] T. Tome and M. J. de Oliveira, *Phys. Rev. Lett.* **108**, 020601 (2012).
- [3] J. Schnakenberg, *Rev. Mod. Phys.* **48**, 571 (1976).
- [4] T. Tome and M. J. de Oliveira, *Phys. Rev. E* **82**, 021120 (2010).
- [5] R. K. P. Zia and B. Schmittmann, *J. Stat. Mech.* (2007) P07012.
- [6] U. Seifert, *Phys. Rev. Lett.* **95**, 040602 (2005).
- [7] T. Tome, *Braz. J. Phys.* **36**, 1285 (2006).
- [8] G. Szabo, T. Tome, and I. Borsos, *Phys. Rev. E* **82**, 011105 (2010).
- [9] B. Gaveau, M. Moreau, and L. S. Schulman, *Phys. Rev. E* **79**, 010102(R) (2009).
- [10] J. L. Lebowitz and H. Spohn, *J. Stat. Phys.* **95**, 333 (1999).
- [11] D. Andrieux and P. Gaspar, *J. Stat. Phys.* **127**, 107 (2007).
- [12] R. J. Harris and G. M. Schutz, *J. Stat. Mech.* (2007) P07020.
- [13] J.-L. Luo, C. Van den Broeck, and G. Nicolis, *Z. Phys. B* **56**, 165 (1984).
- [14] C. Y. Mou, J.-L. Luo, and G. Nicolis, *J. Chem. Phys.* **84**, 7011 (1986).
- [15] C. Maes and K. Netocny, *J. Stat. Phys.* **110**, 269 (2003).
- [16] L. Crochik and T. Tome, *Phys. Rev. E* **72**, 057103 (2005).
- [17] M. Asfaw, *Phys. Rev. E* **89**, 012143 (2014).
- [18] M. A. Taye, *Phys. Rev. E* **92**, 032126 (2015).
- [19] M. A. Taye, *Phys. Rev. E* **94**, 032111 (2016).
- [20] T. Bameta, D. Das, R. Padinhateeri, and M. M. Inamdar, *Phys. Rev. E* **95**, 022406 (2017).
- [21] D. Oriola and J. Casademunt, *Phys. Rev. Lett.* **111**, 048103 (2013).
- [22] O. Campas, Y. Kafri, K. B. Zeldovich, J. Casademunt, and J.-F. Joanny, *Phys. Rev. Lett.* **97**, 038101 (2006).
- [23] K. Brandner, M. Bauer, M. Schmid, and U. Seifert, *New. J. Phys.* **17**, 065006 (2015).
- [24] B. Gaveau, M. Moreau, and L. S. Schulman, *Phys. Rev. E* **82**, 051109 (2010).
- [25] E. Boukobza and D. J. Tannor, *Phys. Rev. Lett.* **98**, 240601 (2007).
- [26] T. Tomé and M. J. de Oliveira, *Phys. Rev. E* **91**, 042140 (2015).
- [27] J. M. Sancho, M. S. Miguel, and D. Duerr, *J. Stat. Phys.* **28**, 291 (1982).
- [28] A. M. Jayannavar and M. C. Mahato, *Pramana J. Phys.* **45**, 369 (1995).
- [29] P. Hänggi, *Helv. Phys. Acta* **51**, 183 (1978).
- [30] P. Hänggi, *Helv. Phys. Acta* **53**, 491 (1980).
- [31] K. Sekimoto, *J. Phys. Soc. Jpn.* **66**, 1234 (1997).
- [32] K. Sekimoto, *Prog. Theor. Phys. Suppl.* **130**, 17 (1998).
- [33] M. Matsuo and S. Sasa, *Physica A* **276**, 188 (2000).
- [34] M. Asfaw, *Eur. Phys. J. B* **86**, 189 (2013).